Total Energy Shaping with Neural Interconnection and Damping Assignment - Passivity Based Control

Santiago Sánchez-Escalonilla   SANTIAGO.SANCHEZ@RUG.NL

Rodolfo Reyes-Báez   R.REYES.BAEZ@RUG.NL

Bayu Jayawardhana   B.JAYAWARDHANA@RUG.NL

Jan C. Willems Center for Systems and Control,
Engineering and Technology Institute Groningen (ENTEG),
Rijksuniversiteit Groningen

Editors: R. Firoozi, N. Mehr, E. Yel, R. Antonova, J. Bohg, M. Schwager, M. Kochenderfer

Abstract

In this work we exploit the universal approximation property of Neural Networks (NNs) to design interconnection and damping assignment (IDA) passivity-based control (PBC) schemes for fully-actuated mechanical systems in the port-Hamiltonian (pH) framework. To that end, we transform the IDA-PBC method into a supervised learning problem that solves the partial differential matching equations, and fulfills equilibrium assignment and Lyapunov stability conditions. A main consequence of this, is that the output of the learning algorithm has a clear control-theoretic interpretation in terms of passivity and Lyapunov stability. The proposed control design methodology is validated for mechanical systems of one and two degrees-of-freedom via numerical simulations.

Keywords: Deep Neural Networks, Physics-informed Machine Learning, Nonlinear Control, Passivity - based Control

1. Introduction

In many nonlinear control techniques the construction of the nonlinear controller is conditioned to the explicit solution of a set of partial differential equations (PDEs) that embed the design requirements, for instance, feedback linearization (Isidori et al., 1995), Lyapunov-based control (Khalil, 2015), and passivity-based control (PBC) (van der Schaft, 2017). The latter approach is a popular technique in practice due to the clear physical interpretation of the control scheme in terms of energy. In this context, the IDA-PBC technique, introduced in Ortega et al. (2002), is a well-known PBC design method for the control of affine nonlinear systems, for which the target closed-loop dynamics take the form of a passive pH system with desired passivity and interconnection properties. A major disadvantage of this method is that to construct the control scheme, it is necessary to solve a set of PDEs, the so-called *matching equations* (MEs), in order to obtain the target pH closed-loop system. While solving these PDEs is non-trivial in general, analytic solutions can be obtained for some classes of systems by restricting the family of target pH systems. We refer interested readers to (Nageshrao et al., 2015) for a review on methods to solve the IDA-PBC PDEs.

In the present paper we propose a method to overcome the problem of finding analytical solutions of the MEs by transforming the IDA-PBC design into a supervised learning problem using NNs where the minimized cost function is systematically constructed to represent the IDA-PBC methodology and port-Hamiltonian systems' first-principles, resulting in a control-informed NN

hereupon referred as Neural IDA-PBC. This is motivated by the universal approximation property of NNs (Hornik et al., 1989; Cybenko, 1989; Kratsios and Papon, 2021). Generally, the main focus of systems & control theory is the analysis of dynamical systems and the design of control input functions, that can steer the system to a desired state satisfying a set of dynamical properties. Correspondingly, it is natural to use NNs as functional surrogates of the control input functions. Yet, for the past decades, the application of NNs in the control (such as in data-driven control) of complex engineering systems is fairly limited due to the lack of explainability of the solution, and their use is oftentimes discouraged. Fortunately, recent progress in the regularization of NNs has allowed us to obtain parametric functions that satisfy predefined restrictions. With the seminal work physics-informed neural networks (PINNs) (Raissi et al., 2017a,b; Karniadakis et al., 2021), it has been shown that constitutive physical laws (in the form of PDEs) can be encoded in the training process, which results in NNs that "understand/respect" the physics of the problem. In other words, during the optimization process, an approximated solution of the underlying physical laws can be obtained.

In the past, researchers have studied different ways of combining learning with control theory. As an example, finding the right Control-Lyapunov function with desirable closed-loop properties (such as large basin of attraction) can be cumbersome and often relies in polynomial approaches that limit the control law to a particular function class. Richards et al. (2018); Chang et al. (2020); Grüne (2020) propose using NNs to learn new families of Lyapunov candidates. Chang and Gao (2021) show how the Lyapunov method can be used to regularize the policy optimization process in Reinforcement Learning, by adding a Lyapunov Critic into the optimization loop. Although the IDA-PBC method is rewritten as an optimization problem, in the present paper, we do not consider any performance metrics over the trajectory. For a review in the connection between optimal control and PBC, the reader is referred to (Fujimoto et al., 2003; Vu and Lefèvre, 2018; Massaroli et al., 2021).

The rest of this paper is divided into 4 sections: Section 2 briefly introduces mechanical systems in the port-Hamiltonian formulation, followed by the IDA-PBC control methodology as presented in Ortega et al. (2002); Section 3 contains the main contribution of this paper, starting from the universal approximation property of NNs, we define a series of residual terms that encode the fundamentals of IDA and PBC; Section 4 numerically validates the Neural IDA-PBC approach; and finally, Section 5 closes with conclusions and future work.

2. Preliminaries

2.1. Mechanical systems in the port-Hamiltonian framework

The dynamics of a standard mechanical system in the pH framework (see van der Schaft (2007)) with generalized coordinates q on the configuration space $\mathcal{Q} \subset \mathbb{R}^n$ and velocity $\dot{q} \in T_q\mathcal{Q}$, is

$$\dot{x} = [J(x) - R(x)]\frac{\partial H}{\partial x}(x) + g(x)u, \qquad y = g^\top(x)\frac{\partial H}{\partial x}(x), \qquad (1)$$

with Hamiltonian function given by the total energy of the system $H(x) = \frac{1}{2}p^\top M^{-1}(q)p + U(q)$, where $x = (q, p) \in \mathcal{X}$ is the state and $p := M(q)\dot{q}$ is the generalized momentum. The scalar function $U(q)$ is the potential energy, and $M(q) = M^\top(q) > 0$ is the inertia matrix. The interconnection, dissipation and input matrices, respectively are given by $J(x) = \begin{bmatrix} 0_n & I_n \\ -I_n & 0_n \end{bmatrix}$, $R(x) = \begin{bmatrix} 0_n & 0_n \\ 0_n & D(x) \end{bmatrix}$, $g(x) = \begin{bmatrix} 0_n \\ B(q) \end{bmatrix}$, where the $n \times n$ matrix $D(x) = D^\top(x) \geq 0_n$ is a dissipation term; and I_n and

0_n are the $n \times n$ identity and zero matrices, respectively. The input u represents generalized forces while the output y gives the generalized velocity so that their inner-product is power. The input force matrix $B(q)$ has rank $m \leq n$. If $n = m$ then the mechanical system in (1) is *fully-actuated*.

The rate of change of $H(x)$ provides a power balance relation between the internal power of system (1) and the external supplied power, the so-called power balance analysis:

$$\dot{H}(x) = \frac{\partial H^\top}{\partial q}(x)\dot{q} + \frac{\partial H^\top}{\partial p}(x)\dot{p} = -\frac{\partial H^\top}{\partial p}(x)D(x)\frac{\partial H}{\partial p}(x) + y^\top u \leq y^\top u. \qquad (2)$$

where the inner-product $y^\top u$ is the external supplied power. In the context of *dissipativity theory*, the inequality in (2) shows that the map $u \mapsto y$ is *passive* with respect to the storage function given by the Hamiltonian function H and the supply rate $y^\top u$. The interested reader is referred to (van der Schaft, 2017, Section 6.2) for a detailed treatment on passivity.

2.2. Interconnection and Damping Assignment Passivity-based Control (IDA-PBC)

The IDA-PBC nonlinear technique, as proposed in (Ortega et al., 2002), is a passivity-based control design method whose main control objective is to design a *static* state feedback control law of the form $u(x) = \beta(x) + v$ for the pH system in (1), such that the closed-loop dynamics is given by the target passive pH system

$$\dot{x} = [J_d(x) - R_d(x)]\frac{\partial H_d}{\partial x}(x) + g(x)v, \qquad y' = g(x)^\top\frac{\partial H_d}{\partial x}(x), \qquad (3)$$

where $J_d(x) = -J_d^\top(x)$ and $R_d(x) = R_d^\top(x) \geq 0$ are the *desired* interconnection and damping matrices, respectively; and $H_d(x)$ is the desired energy function. The desired Hamiltonian function $H_d(x)$ has a strict local minimum at the desired equilibrium point $x^\star = (q^\star, 0)$ and the tuple (v, y') is the new power conjugate pair that defines the desired passivity relation with storage function $H_d(x)$.

The main result in Ortega et al. (2002) is the following:

Theorem 1 (IDA-PBC) *Consider $J(x), R(x), H(x), g(x)$ of the pH system in (1) and the desired equilibrium to be stabilized $x^* \in \mathcal{X}$. Assume that there exists functions $J_d(x), R_d(x)$ and $H_d(x)$ satisfying the* matching equation

$$g^\perp(x)[J_d(x) - R_d(x)]\frac{\partial H_d}{\partial x}(x) = g^\perp(x)[J(x) - R(x)]\frac{\partial H}{\partial x}(x), \qquad (4)$$

where $g^\perp(x)$ is the full rank left annihilator of $g(x)$. Then the control law

$$u = \underbrace{[g^\top(x)g(x)]^{-1}g^\top(x)\left((J_d(x) - R_d(x))\frac{\partial H_d}{\partial x}(x) - (J(x) - R(x))\frac{\partial H}{\partial x}(x)\right)}_{\beta(x)} + v \qquad (5)$$

locally stabilizes system (1) and the closed-loop system (3) is passive with the new input v and output y. Moreover, if x^* is the largest invariant subset in $\{x \in \mathcal{X} | \frac{\partial H_d^\top}{\partial x}(x)R_d(x)\frac{\partial H_d}{\partial x}(x) = 0\}$ then x^* is asymptotically stable. The results holds globally if x^* is a global minimum of $H_d(x)$ and $H_d(x)$ radially unbounded.

After some straightforward algebraic manipulations, it is easy to show that the desired functions can be rewritten as the sum of the functions $J(x), R(x), H(x)$ of the pH system in (1) and some *auxiliary* functions $J_a(x), R_a(x), H_a(x)$ such that

$$J_d(x) := J(x) + J_a(x), \quad R_d(x) := R(x) + R_a(x) \quad H_d(x) := H(x) + H_a(x). \tag{6}$$

These auxiliary terms are used to *assign* the desired functions in Theorem 1. Some implicit design requirements in Theorem 1 are mentioned below as these are key for the constructive procedure that will be presented in Section 3.

(P1) <u>Structure preservation</u>: the matrices $[J(x) + J_a(x)]$ and $[R(x) + R_a(x)] \geq 0$ are skew-symmetric and symmetric, respectively.

(P2) <u>Integrability</u>: $K(x) = \frac{\partial H_a}{\partial x}(x)$ is the gradient of a scalar function, i.e. $\frac{\partial K}{\partial x}(x) = \left[\frac{\partial K}{\partial x}(x)\right]^\top$.

(P3) <u>Equilibrium assignment</u>: $\frac{\partial H_d}{\partial x}(x^\star) = \frac{\partial H}{\partial x}(x^\star) + \frac{\partial H_a}{\partial x}(x^\star) = 0$, where $x^\star = \text{argmin}_{x \in \Omega} H_d(x)$.

(P4) <u>Lyapunov stability</u> $H_d(x)$ is a positive definite function at $x^\star$, e.g. $\frac{\partial^2 H}{\partial x^2}(x^\star) + \frac{\partial^2 H_a}{\partial x^2}(x^\star) > 0$.

Under these conditions, the closed-loop system will be a PCH system with the form (3), where $H_d(x)$ is the closed-loop energy function.

3. Neural IDA-PBC

In this section we introduce how Neural Networks can be used to solve the PDEs in (4). This methodology is based on the intrinsic property of Neural Networks as Universal Approximators (Hornik et al., 1989; Cybenko, 1989; Kratsios and Papon, 2021).

3.1. Using PINNs to solve PDEs

As showcased in (Raissi et al., 2017a,b), the universal approximation property of NNs can be exploited to find the solution of ill-posed problems such as the ones involving PDEs. Considering a nonlinear parametric partial differential equation of the form

$$u_t + \mathcal{N}[u; \lambda] = 0, \tag{7}$$

where $\mathcal{N}[\cdot; \lambda]$ is a nonlinear operator parameterized by λ and u_t is the time derivative of the function $u(t, x)$. We can define a residual term, $f(t, x)$, as the left-hand-side of (7) such that the NN that minimizes this residual is considered an approximated solution of (7), i.e.

$$\mathcal{L}(\theta; x) := u_t(\theta; t, x) + \mathcal{N}[u(\theta; t, x); \lambda], \qquad \theta^\star = \text{argmin}_\theta \mathcal{L}(\theta; x). \tag{8}$$

In this case, $u(t, x) = u_\theta(\theta^\star; t, x) + \epsilon$, and the result is a deep neural network that encodes the relation(s) of PDE(s). This methodology is known as *Physics Informed Neural Networks (PINNs)*.

3.2. Using PINNs to solve the non-parameterized IDA-PBC

Assuming the existence of solutions for the problem defined by (4), (P1) - (P4), finding the missing functions $J_a(x)$, $R_a(x)$ and $H_a(x)$ is an inverse problem, in particular an ill-posed one, which makes it a perfect candidate to be studied under the scope of physics-informed machine learning (Karniadakis et al., 2021).

To reduce the underdeterminism of the problem, we adopt the non-parameterized IDA-PBC approach, formalized in (Nageshrao et al., 2015), which requires solving the MEs after fixing the choice of $J_d(x)$ and $R_d(x)$. However, in order to avoid triviality when choosing these values, we propose to only fix $J_d(x)$, while iteratively adapting $R_d(x)$ to obtain certain desired properties of the closed-loop system. At the same time, $H_d(x) := H(x) + H_a(x)$ can be approximated using NNs. The diagram in Figure 1 illustrates this working strategy.
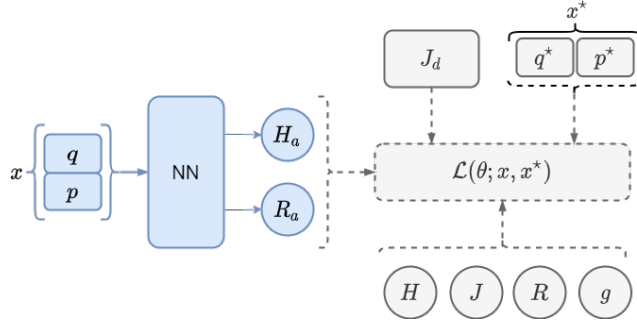

Figure 1: Neural IDA-PBC diagram. The NN is used to solve the non-parameterized IDA-PBC problem. It approximates the auxiliary energy and damping functions, H_a, and R_a, such that the loss function $\mathcal{L}(\theta; x, x^\star)$ is minimized. This loss function is methodologically constructed in Section 3.3. x is a tuple of points in the state space $\mathcal{X}$. H, J, R and g are the open loop Hamiltonian, interconnection, damping and input matrices as in Section 2.1. The desired interconnection matrix $J_d(x)$ and desired equilibrium point $x^\star$ are fixed and passed directly into the loss function.

3.3. IDA-PBC loss function

This section defines the residuals that encode the IDA-PBC principles listed in Section 2.2. They are then combined into the objective function needed to be minimized using NNs. For simplicity in the presentation, we will only consider fully-actuated mechanical systems given by (1) with the standard Hamiltonian function H. The residuals are created from (P1) - (P4) as follows.

(P1) Structure preservation residual

Interconnection matrix   In order to satisfy this property we are forced to choose an auxiliary interconnection matrix $J_a(x)$ with a skew-symmetric form. Correspondingly, we consider the following structure for J_a as proposed in (Ortega and Spong, 2000), $J_a(x) = \begin{bmatrix} 0 & J_1(x) \\ -J_1(x)^\top & J_2(x) \end{bmatrix}$, where $J_1(x)$ is an arbitrary $n \times n$ matrix and $J_2(x) \in \mathbb{R}^{n \times n}$ is skew-symmetric matrix. Both are fixed by the user prior to the optimization process.

Dissipation matrix The desired damping matrix R_d in (P1) must be positive semi-definite. For this matrix, we also choose to adopt the parametric version of the structure in (Ortega and Spong, 2000), $R_a(\theta; x) = \begin{bmatrix} 0 & 0 \\ 0 & R_2(\theta;x) \end{bmatrix}$, where $R_2(\theta; x) \in \mathbb{R}^{n \times n}$ is symmetric and positive-definite matrix parametrized by θ. The parameterization of R_a is to enable the discovery of admissible damping functions that fulfill the design criteria during the optimization process. For instance, the chosen criteria is related to the transient behavior of the closed-loop system, where we can prescribe the transient behaviour through the enforcement of the rate of energy decrease via $F_d(x) = J_d(x) - R_d(x)$. In particular, we define the following residual

$$f_{\text{transient}}(\theta; x) := \underbrace{\max\left\{0, c + \text{Re}(\sigma(F_d(x)))\right\}}_{f_{\text{damping}}} + \underbrace{\|\text{Im}(\sigma(F_d(x)))\|}_{f_{\text{harmonic}}}, \tag{9}$$

where $c > 0$ is the prescribed convergence rate of the new energy function H_d, Re and Im are the real and imaginary part, respectively. The first term is related to the residual for prescribing the damping of target system while the second term corresponds to the residual for minimizing the harmonic oscillation.

(P2) Integrability residual As the NNs are used to obtain the scalar function $H_a(\theta; x)$, the integrability condition (P2) is fulfilled by construction.

(P3) Equilibrium assignment residual The condition in (P3) implies that the closed-loop energy function, has a global minimum at the desired equilibrium $x^\star = (q^\star, 0)$. Correspondingly, we consider the following residual function to assign the equilibrium point

$$f_{\text{eq}}(\theta; x, x^*) := \underbrace{\left\|\frac{\partial H_d}{\partial x}(\theta; x^\star)\right\|^2}_{f_{\text{eq},1}} + \underbrace{(H_d(\theta; x^\star))^2 + \max\{0, -H_d(\theta; x)\}}_{f_{\text{eq},2}}, \tag{10}$$

where $f_{\text{eq},1}$ defines that x^* is a stationary point and $f_{\text{eq},2}$ is used to induce a lower bound on H_d.

(P4) Lyapunov stability residual This condition is equivalent to having the spectrum of $\frac{\partial^2 H_d}{\partial x^2}(\theta; x)$ to be positive. Therefore the residual function to guarantee (P4) is given by

$$f_{\text{lyap}} := \max\left\{0, c - \sigma(H_d(\theta; x))\right\}, \tag{11}$$

where σ denotes the spectrum of a matrix and $c > 0$ is again a constant value that can be added to make this condition stricter.

IDA-PBC matching equation residual We can rewrite the IDA-PBC ME (4) in the residual form moving all the terms to the left-hand-side as it is presented in 3.1,

$$f_{\text{matching}} := g^\perp(x)[J_d(x) - R_d(x)]\frac{\partial H_d}{\partial x}(x) - g^\perp(x)[J(x) - R(x)]\frac{\partial H}{\partial x}(x). \tag{12}$$

Finally, we can combine all residuals (9) - (12) to get the final cost function

$$\mathcal{L} = f_{\text{transient}} + f_{\text{eq}} + f_{\text{lyap}} + f_{\text{matching}}. \tag{13}$$

This cost function implicitly encodes the family of admissible solutions of the IDA-PBC control scheme. As a consequence of the universal approximation theorem (Hornik et al., 1989; Cybenko, 1989), if follows that the NN that minimizes (13) approximates the required auxiliary functions $R_a^\star(x) \approx R_a(\theta^\star; x) + \epsilon$ and $H_a^\star(x) \approx H_a(\theta^\star; x) + \epsilon$, that asymptotically stabilize the system at the desired equilibrium point $x^\star$.

4. Neural IDA-PBC for mechanical systems

This section includes the numerical results for two different examples. The NN used throughout this section has 3 hidden layers of 20 units each, and the optimizer chosen is Adam with a learning rate of 0.001, that is interrupted after certain convergence tolerance is reached, followed by L-BFGS-B as presented in the seminal work (Raissi et al., 2017a).
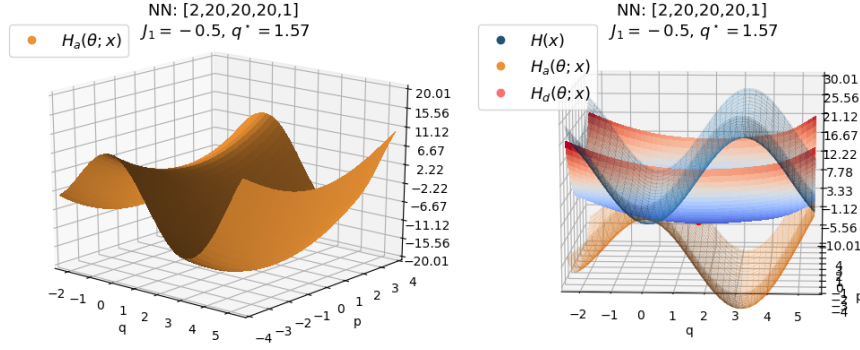
4.1. Simple Pendulum

The simple pendulum is a well established example in robotics due to its non-linear dynamics and simple formulation. In this case we consider a system with no natural damping, actuated at its joint i.e. $g(x) = \begin{bmatrix} 0 & 1 \end{bmatrix}^\top$, to be stabilized at an arbitrary configuration $x^\star = (q^\star, 0)$. The total energy of this system is given by $H(x) = \frac{1}{2ml^2}p^2 + mgl(1 - \cos q)$.

Substituting into (4), we obtain the ME for this problem $(1 + J_1)\frac{\partial H_a}{\partial p}(x) = -J_1\frac{\partial H}{\partial p}$, which together with (P1) - (P4) encode the family of solutions defined by the IDA-PBC control methodology. In Figures 2 and 3 we present the numerical results for two illustrative cases where $J_1 = -0.5$ and $J_1 = 1$ respectively. The choice of these values can be intuitively interpreted changing the closed-loop inertia by a factor of two.

In both cases we observe that the NN is able to approximate the required $H_a(x)$ and $R_a(x)$, therefore asymptotically stabilizing the closed-loop system at the desired point $x^\star = (\pi/2, 0)$. Additionally, Figures 2(b) and 3(b) show a comparison of $q(t)$ and $p(t)$ between Neural IDA-PBC methodology for a non-trivial $J_a(x)$ and the solution of IDA-PBC when $J_1 = 0$ is chosen to simplify the original MEs (pure potential energy compensation). From this comparison, it is evident that although (in the simple pendulum case) modifying the kinetic energy of the system is not crucial for stabilization, being able to solve the MEs for non-arbitrary choices of $Ja(x)$ is important to not limit the energy-based controller to a particular family of solutions where the trajectory might be sub-optimal.

4.2. Double Pendulum

The double pendulum system is also very common in robotics and it is normally used to represent a 2-link manipulator. In this example we also consider that there is no natural damping on the system, that the actuation also occurs at its joints, i.e. $g(x) = \begin{bmatrix} 0_{2\times2} & I_2 \end{bmatrix}^\top$ and we want to stabilize the system at $x^\star = (q_1^\star, q_2^\star, 0, 0)$. The total energy function for this system is given by $H(q, p) = \frac{1}{2}\begin{bmatrix} p_1 & p_2 \end{bmatrix} M^{-1}(q)\begin{bmatrix} p_1 \\ p_2 \end{bmatrix} + (m_1 + m_2)gl_1(1 - \cos(q_1)) + m_2gl_2(1 - \cos(q_2))$ where the inertia matrix $M(q)$ is given by $M(q) = \begin{bmatrix} (m_1+m_2)l_1^2 & m_2l_1l_2\cos(q_1-q_2) \\ m_2l_1l_2\cos(q_1-q_2) & m_2l_2^2 \end{bmatrix}$.

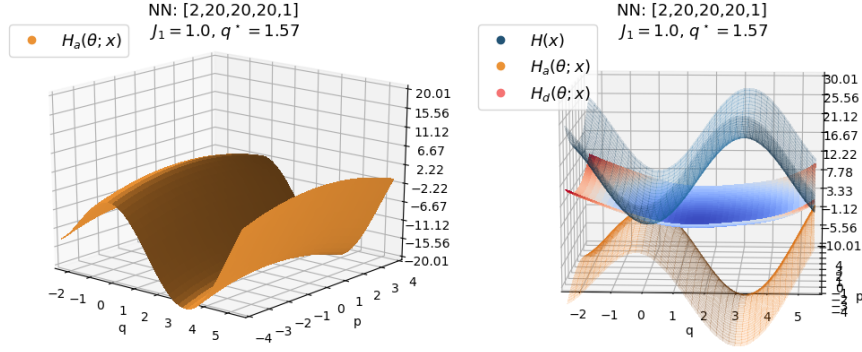(a) Potential maps of different energy functions for $J_1 = \mathrm{diag}(-0.5)$.
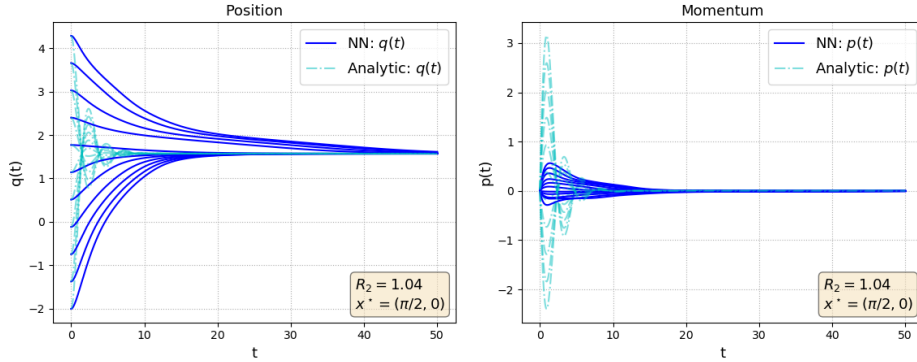
(b) Temporal dynamics of q (left) and p (right) for different initial conditions.

Figure 2: Numerical simulations of the simple pendulum system for different values of $J_a(x)$ parameterized as in (P1): (a) On the left, the approximated $H_a(\theta; x)$ that satisfies the simple pendulum matching equations when $J_1 = \mathrm{diag}(-0.5)$. On the right, the resulting closed-loop energy function $H_d(\theta; x) = H(x) + H_a(\theta; x)$ (solid curve) which is convex and has a minimum at $x^\star = (\pi/2, 0)$; (b) Neural IDA-PBC (solid line) after fixing $J_1 = -0.5$ vs the analytical solution of the MEs (dashed line) when $J_a(x) = 0$ and the potential energy is compensated to be quadratic around $x^\star$.

In this case, substituting into (4), we obtain two MEs that need to be satisfied in order to obtain an IDA-PBC control law that stabilizes the system:

$$(1 + J_{11})\frac{\partial H_a}{\partial p_1}H_a(x) = -J_{11}\frac{\partial H_a}{\partial p_1}(x) \quad \text{and} \quad (1 + J_{12})\frac{\partial H_a}{\partial p_2}(x) = -J_{12}\frac{\partial H_a}{\partial p_2}(x).$$

Notice that these MEs, only impose a structure in the generalized momenta directions. Therefore, in order to ease the discovery of the solution using NNs, we create an additional complementary residual to steer the closed-loop system in the generalized coordinates direction. Suppose $H_d(x) = \frac{1}{2}p^\top N(q)p + U_d(q - q^\star)$, where $N(q)$ is a positive definite matrix, then the gradient in the coordinates direction $\frac{\partial H_d}{\partial q}(x) = F(q, p) + \frac{\partial U_d}{\partial q}(q - q^\star) \approx G_d(q - q^\star)$ must be a monotonic function to guarantee the Lyapunov stability condition (P4). We can choose this function apriori, by

(*a*) Potential maps of different energy functions for $J_1 = \text{diag}(1.0)$.
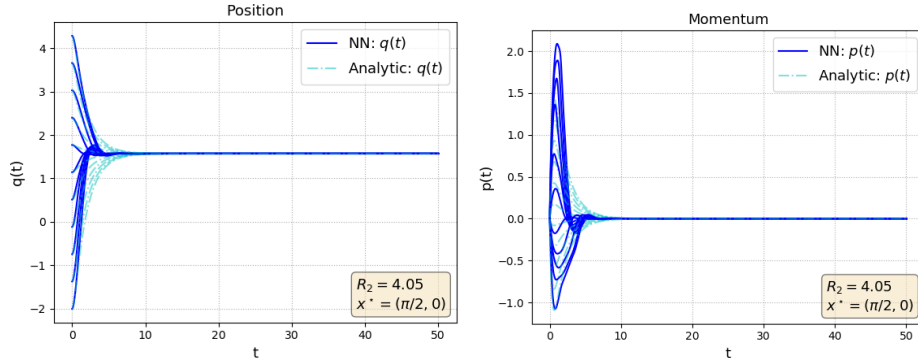
(*b*) Temporal dynamics of q (left) and p (right) for different initial conditions.

Figure 3: Numerical simulations of the simple pendulum system for different values of $J_a(x)$ parameterized as in (P1): (a) On the left, the approximated $H_a(\theta; x)$ that satisfies the simple pendulum matching equations when $J_1 = \text{diag}(1.0)$. On the right, the resulting closed-loop energy function $H_d(\theta; x) = H(x) + H_a(\theta; x)$ (solid curve) which is convex and has a minimum at $x^\star = (\pi/2, 0)$; (b) Neural IDA-PBC (solid line) after fixing $J_1 = 1.0$ vs the analytical solution of the MEs (dashed line) when $J_a(x) = 0$ and the potential energy is compensated to be quadratic around $x^\star$.

defining a complementary residual as

$$f_{\text{comp}}(\theta; x, x^*) := G_d(q - q^\star) - \left(\frac{\partial H}{\partial q}(x) + \frac{\partial H_a}{\partial q}(\theta; x) \right)$$

$$\mathcal{L} = f_{\text{transient}} + f_{\text{eq}} + f_{\text{lyap}} + f_{\text{matching}} + \lambda f_{\text{comp}}$$

where λ is an extra multiplier that can be adjusted to change the closed-loop temporal dynamics.

In Figure 4 we present the temporal dynamics of $q(t)$ and $p(t)$ for two different cases ($J_1 = \text{diag}(-0.5), J_2 = 0$) and ($J_1 = \text{diag}(1.0), J_2 = 0$). Here, we also compare the Neural IDA-PBC response with the case where $J_a(x) = 0$ (pure potential energy compensation). We can see that the Neural IDA-PBC method is capable of asymptotically stabilizing the system around a desired point. And again, the comparison with the pure potential energy compensation case (as it is commonly done in practice), shows how modifying the closed-loop interconnection matrix has a big impact in the closed-loop system trajectories.
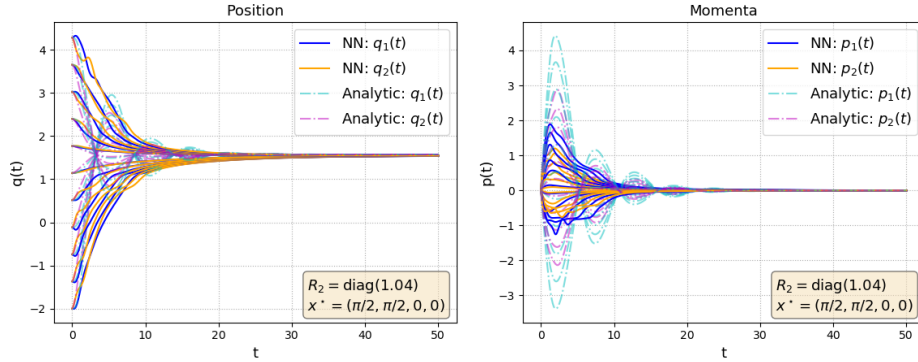
(*a*) The temporal dynamics of q (left) and p (right) for different initial conditions.
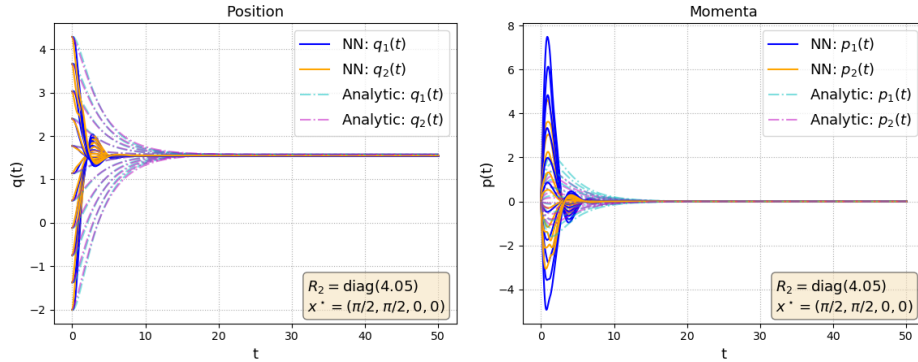
(*b*) The temporal dynamics of q (left) and p (right) for different initial conditions.

Figure 4: Numerical simulations of the double pendulum system for different values of $J_a(x)$ parameterized as in (P1): (a) Neural IDA-PBC (solid line) after fixing the pair ($J_1 = \text{diag}(-0.5)$, $J_2 = 0$) vs the analytical solution of the MEs (dashed line) when $J_a(x) = 0$ and the potential energy is compensated to be quadratic around $x^\star$; (b) Neural IDA-PBC (solid line) after fixing the pair ($J_1 = \text{diag}(1.0)$, $J_2 = 0$) vs the analytical solution of the MEs (dashed line) when $J_a(x) = 0$ and the potential energy is compensated to be quadratic around $x^\star$.

5. Conclusions

In this paper we have presented a systematic approach to solve the IDA-PBC problem formulation using control-informed neural networks. For this purpose we have adapted the residual methodology presented in (Karniadakis et al., 2021) to cover the fundamentals required by the IDA control method and the PBC theory. Despite the fact that fully-actuated systems do not require kinetic energy-shaping for stabilization purposes, the simulation results show that modifying the kinetic energy is beneficial to improve the transient behavior. However, finding the controller that achieves this and satisfies the MEs can be very hard due to the nonlinearities and coupled dynamics of the system under study. The main advantage of Neural IDA-PBC is that it enables finding approximations to this type of controllers thanks to the automatic discovery of solutions to the MEs.

Conclusively, the presented methodology enables the derivation of *total energy shaping controllers* that allow exploiting the true physics of the system without the need of taking *restrictive* mathematical assumptions to ease the calculations.

Acknowledgments

References

Ya-Chien Chang and Sicun Gao. Stabilizing Neural Control Using Self-Learned Almost Lyapunov Critics. *arXiv:2107.04989*, July 2021.

Ya-Chien Chang, Nima Roohi, and Sicun Gao. Neural Lyapunov Control. *arXiv:2005.00611*, December 2020.

G. Cybenko. Approximation by superpositions of a sigmoidal function. *Math. Control Signal Systems*, 2(4):303–314, December 1989.

K. Fujimoto, T. Horiuchi, and T. Sugie. Optimal control of Hamiltonian systems with input constraints via iterative learning. In *42nd IEEE International Conference on Decision and Control*, pages 4387–4392, 2003.

Lars Grüne. Computing Lyapunov functions using deep neural networks. *arXiv:2005.08965*, November 2020.

Kurt Hornik, Maxwell Stinchcombe, and Halbert White. Multilayer feedforward networks are universal approximators. *Neural Networks*, 2(5):359–366, January 1989.

Alberto Isidori, ED Sontag, and M Thoma. *Nonlinear control systems*, volume 3. Springer, 1995.

George Em Karniadakis, Ioannis G. Kevrekidis, Lu Lu, Paris Perdikaris, Sifan Wang, and Liu Yang. Physics-informed machine learning. *Nat Rev Phys*, 3(6):422–440, June 2021.

Hassan K. Khalil. *Nonlinear control*. Pearson, Boston, 2015.

Anastasis Kratsios and Leonie Papon. Universal Approximation Theorems for Differentiable Geometric Deep Learning. *arXiv:2101.05390*, June 2021.

Stefano Massaroli, Michael Poli, Federico Califano, Jinkyoo Park, Atsushi Yamashita, and Hajime Asama. Optimal Energy Shaping via Neural Approximators. *arXiv:2101.05537*, January 2021.

S P Nageshrao, G A D Lopes, D Jeltsema, and R Babuška. Adaptive and Learning Control of port-Hamiltonian Systems: A Survey. *IEEE Transactions on Automatic Control*, page 37, 2015.

Romeo Ortega and Mark W. Spong. Stabilization of Underactuated Mechanical Systems Via Interconnection and Damping Assignment. *IFAC Proceedings Volumes*, 33(2):69–74, March 2000.

Romeo Ortega, Arjan van der Schaft, Bernhard Maschke, and Gerardo Escobar. Interconnection and damping assignment passivity-based control of port-controlled Hamiltonian systems. *Automatica*, 38(4):585–596, April 2002.

Maziar Raissi, Paris Perdikaris, and George Em Karniadakis. Physics Informed Deep Learning (Part I): Data-driven Solutions of Nonlinear Partial Differential Equations. *arXiv:1711.10561*, November 2017a.

Maziar Raissi, Paris Perdikaris, and George Em Karniadakis. Physics Informed Deep Learning (Part II): Data-driven Discovery of Nonlinear Partial Differential Equations. *arXiv:1711.10566*, November 2017b.

Spencer M. Richards, Felix Berkenkamp, and Andreas Krause. The Lyapunov Neural Network: Adaptive Stability Certification for Safe Learning of Dynamical Systems. *arXiv:1808.00924*, October 2018.

Arjan van der Schaft. Port-Hamiltonian systems: an introductory survey. In *Proceedings of the International Congress of Mathematicians*, pages 1339–1365. European Mathematical Society Publishing House, May 2007.

Arjan van der Schaft. *L2-Gain and Passivity Techniques in Nonlinear Control*. Springer International Publishing, 2017.

N. M. Trang Vu and L. Lefèvre. A connection between optimal control and IDA-PBC design. *IFAC-PapersOnLine*, 51(3):205–210, January 2018.